Inhibition of epithelial phosphate transport by NAD^+/NADH.

Susana Lucea, Natalia Guillén, Cecilia Sosa and Víctor Sorribas[1*]

1 Group of Molecular Toxicology, Department of Biochemistry and Molecular and Cell Biology. University of Zaragoza, Veterinary Faculty. Calle Miguel Servet, 177. 50013 Zaragoza (Spain)

* Corresponding author. E-mail: sorribas@unizar.es. ORCID: 0000-0003-3457-323X

Author contributions:

Conceptualization: V.S.

Methodology: S.L., N.G., C.S., V.S.

Software: S.L., V.S., NG

Formal analysis: S.L.,V.S.

Writing—original draft preparation: V.S.

Writing—review and editing: S.L., N.G., C.S.

Funding acquisition: V.S.

All authors have read and agreed to the published version of the manuscript.

Running head: NAD^+/NADH inhibition of Pi transport

ABSTRACT

Nicotinamide is an important regulator of Pi homeostasis after conversion into NAD^+/NADH. In this work, we have studied the classical inhibition of Pi transport by these compounds in the brush border membrane vesicles (BBMV) of rat kidney and rat intestine, and we examined the effects in Opossum Kidney (OK) cells and in phosphate transporter-expressing *Xenopus laevis* oocytes. In BBMV, NAD^+ required preincubation at either room temperature or on ice to inhibit Pi uptake in BBMV. However, no effects were observed in the known Slc34 or Slc20 Pi transporters expressed in *Xenopus* oocytes, in OK cells, or in isolated rat cortical nephron segments. In BBMV from jejunum or kidney cortex, the inhibition of Pi transport was specific, dose-related, and followed a competitive inhibition pattern, as shown by linear transformation and non-linear regression analyses. A K_i value of 538 μM NAD^+ in kidney BBMV was obtained. Ribosylation inhibitors and ribosylation assays revealed no evidence that this reaction was responsible for inhibiting Pi transport. An analysis of the persistence of NAD^+/NADH revealed a half-life of just 2 minutes during preincubation. Out of several metabolites of NAD degradation, only ADP-ribose was able to inhibit Pi uptake. Pi concentration also increased during 30 minutes of preincubation, up to 0.67mM, most likely as a metabolic end-product. In conclusion, the classical inhibition of Pi transport by NAD^+/NADH in BBMV seems to be caused by the degradation metabolites of these compounds during the preincubation time.

KEYWORDS

NAD^+; NADH; nicotinamide; phosphate transport; phosphate homeostasis; inhibitor

ABBREVIATIONS

3-MB: 3-Methoxybenzamide
ADP-R: Adenosine diphosphate ribose
ART: ADP-ribosyltransferases
ARTC: ADP-ribosyltransferase type C
BBMV: brush border membrane vesicles
MIBG: meta-iodobenzylguanidine
NAM: Nicotinamide
NAD^+/NADH, nicotinamide adenine dinucleotide (NAD^+), and the reduced version (NADH)
Nampt: Nicotinamide phosphoribosyltransferase
OK cells: Opossum Kidney cells
PVDF: Polyvinylidene Fluoride

INTRODUCTION

The control of inorganic phosphate (Pi) homeostasis has been the subject of intense research for several decades, given that it involves a complex network of hormonal and non-hormonal mechanisms. The complexity of that network stems from the presence of two substrates ($HPO_4^{=}$ and $H_2PO_4^-$), which are carried by several transporters located mainly in the small intestine and in the kidney proximal tubule; from the many physiological and molecular roles of Pi; and from the severity of the two dysregulation outcomes (hypo- and hyperphosphatemia). Table 1 summarizes the main control mechanisms, but readers are invited to consult more specific texts [1, 2].

The molecular cloning of transporters that are the targets of the main regulatory mechanisms of Pi homeostasis has led to the important findings that are summarized in the special issue of *Pflügers Archiv* (Volume 471, issue 1), commemorating the 25th anniversary of the expression-cloning of the renal sodium-phosphate cotransporter NaPi-IIa [3]. This transporter is mainly expressed in the brush-border membrane of proximal tubular epithelial cells, and it belongs to the Slc34 family of phosphate transporters, whose code is Slc34a1. The other two members of this family are NaPi-IIb (Slc34a2) [4], which is primarily expressed in the intestine and lungs, and the growth-related renal transporter NaPi-IIc (Slc34a3) [5]. All three members of the Slc34 family correspond to type II Pi transporters. Other known sodium-activated Pi cotransporters that were first identified as retrovirus receptors are PiT-1 and PiT-2, belonging to the Slc20 family (Slc20a1 and Slc20a2, respectively) or type III, and they exhibit a less restricted tissue distribution [6, 7].

When renal damage impairs Pi excretion, dietary Pi absorption can exceed the excretion rate. At this point, when phosphaturic mechanisms do not compensate for the Pi intake, Pi homeostasis is lost and hyperphosphatemia is observed, causing further renal damage to the remaining functional nephrons [8, 9]. A series of hormonal, metabolic, and cellular changes will occur in response to the renal damage, to the relative dietary Pi excess, and to the hyperphosphatemia, ending in heart damage and vascular calcification, among other problems. In order to reduce the intestinal absorption rate of Pi, phosphate binders and several Pi transport inhibitors are being developed, with varying therapeutic success [10, 11]. Among those inhibitors, nicotinamide-containing compounds, nicotinamide adenine dinucleotide (NAD^+), and the reduced version, NADH, show very interesting and promising characteristics (Figure 1).

Nicotinamide (NAM) is one of the three vitamers of vitamin B_3 (together with nicotinic acid and nicotinamide riboside). It is mainly synthesized in the liver from L-tryptophan, although also from niacin, and it is subsequently released into the blood and used by peripheral tissues to produce NAD^+ [12]. The liver also generates NAD^+ directly from L-tryptophan or from nicotinic acid, but in mammals the predominant precursor is NAM through the salvage pathway where nicotinamide phosphoribosyltransferase (Nampt) is the rate-limiting enzyme. The release of NAM and its conversion into NAD^+ through the Nampt/NAD^+ system seems to be responsible for the daily oscillations in phosphatemia as a result of modifying the abundances of the active Slc34 Pi transporters [13, 14]. While there are many unsolved questions regarding the inhibitory mechanisms of

these compounds, two main mechanisms have been suggested: a direct competitive inhibition by NAD^+ and NADH described in brush-border membrane vesicles (BBMV) from kidney cortex [15,16], and an indirect, non-competitive inhibition of renal [16] and intestinal Pi transport by NAM [17] through various cellular mechanisms. By acting on the intestine, NAM is also able to reduce hyperphosphatemia in the experimental adenine-induced CKD model in rats [18]. The non-competitive, inhibitory mechanisms of NAM on Pi transport inhibition seem to be mediated by the increased generation of NAD^+ through Nampt activity [13, 14], while previous works had discarded this possibility and had instead indicated an increased cAMP content in renal proximal tubule suspensions [19, 20] or even an oxidative effect and redox status modification [21].

NAM is also able to increase phosphaturia in animals that are dietary Pi-deprived [22]. During such deprivation, the phosphaturic effects of the parathyroid hormone (PTH) and calcitonin are blunted, but NAM is able to restore the actions of PTH and calcitonin. A subsequent work reported that NAM was mainly acting on the loop of Henle rather than in the proximal tubule and that the inhibitory action of NAM also took place in the convoluted proximal tubules only during Pi deprivation [23].

The competitive inhibition of NAD^+ and NADH was only observed in BBMV from kidney cortex, when the compounds were incubated directly with the vesicles [16]. However, using this experimental setup, NAM had no effect on Pi uptake [15], and most importantly, the inhibitory effect of NAD^+/NADH in BBMV was dose-related, using concentrations of NAD^+/NADH in the micromolar, physiological range. In BBMV, NAD^+/NADH truly binds the vesicles rather than acting intravesicularly after uptake of the nucleotides, with a Kd that is also in the micromolar range [24].

Direct and competitive inhibition in BBMV was surprising because the chemical structure of Pi and NAD^+/NADH are completely different. In this work, we studied the phenomenon again, with the main objectives of revisiting the kinetic mechanisms of inhibition using non-linear regression methods, analyzing which of the known Pi transporters are the target of competitive inhibition in the heterologous expression system of *Xenopus laevis* oocytes, verifying if ribosylation is the reaction that is responsible for the NAD^+/NADH inhibition of Pi transport, and checking whether inhibition is performed directly by NAD^+/NADH or by any of the likely metabolites.

MATERIALS AND METHODS

All the animals used in this work were cared for in accordance with European and Spanish legislation, and all procedures were approved by the Ethical Committee for Animal Experimentation of the University of Zaragoza, with authorization number PI39/15.

Preparation of membrane vesicles from rat, and transport assays

Two-month-old, male Wistar rats were purchased from Janvier Laboratories (Saint Berthevin Cedex, France) and were fed a control, Teklad 2014 maintenance fodder for rodents containing 0.6% phosphorus. Only males were used to reproduce the original experiments [15-18]. The rats were anesthetized and euthanized by an intraperitoneal injection of tiophental. The small intestines and kidneys were subsequently removed, and the heart was cut for exanguination. Membrane vesicles were prepared from kidney cortex and jejunum scrapings from the rats, as described, using the classic procedure of double magnesium precipitation [25-27]. ^{32}P-Pi uptake was determined by rapid filtration, as described [27]. NAM, NAD^+, and NADH were dissolved in water and mixed with the BBMV (5 μl per experimental point) for preincubation, either at room temperature or on ice. The uptake medium (45 μl) contained the corresponding inhibitor at the same concentration as in preincubation.

Isolation of renal proximal tubules

Proximal tubules were obtained by collagenase digestion, as described in detail [28]. Kidney cortex was obtained manually, as in the preparation of membrane vesicles. The cell viability of cortical segments was confirmed with trypan blue exclusion before beginning treatment with NAD^+. Segments of both kidneys were pooled and then divided for control and treatment. The segments were then incubated for 30 minutes with 0.5 mM NAD^+ in cell uptake medium, similarly to OK cells (see below), and BBMV were then immediately prepared. Due to the small amount of starting material, proximal tubule homogenization was performed manually using a syringe with a 25g needle.

Preparation and use of *X. laevis* oocytes, and in vitro transcriptions

Xenopus females were purchased from the European Xenopus Resource Centre of the University of Portsmouth (Portsmouth, UK) and were maintained in the standard conditions for this species, in large dark water tanks at 18º C. Oocytes were obtained by abdominal incision after anesthesia with MS222 and bupivacaine for analgesia.

The rat NaPi-IIa and NaPi-IIb cDNAs used were the originals cloned by functional expression [3, 4]. NaPi-IIc and PiT2 were PCR-cloned from retrotranscribed RNA from rat kidney cortex using the primers TCCATCGCTTTCCAGAGCAG and TGGCTGAGTTCTAAGCTCGC for PiT2 and ACATGCAGATCTAGGATTGGGC and AAAGGAGAGGATGCAGAGAC for NaPi-IIc. They were inserted in pCR4-TOPO and sequenced. Rat PiT1 was cloned and used as previously reported [29]. After linearizing the plasmids at the 3'

ends of the cDNAs, they were *in vitro*-transcribed, capped, polyadenylated, and purified using mMESSAGE mMACHINE and Poly(A) Tailing Kits, both from Invitrogen (Carlsbad, CA, USA). The injection, handling of oocytes, and uptake assays of ^{32}Pi were performed as described [29,30].

Culture and Pi uptake assays in OK cells

The culture of Opossum Kidney cells and the procedure for determining the Pi uptake in this cell line have been described in many articles [31].

Quantification of NAD^+/NADH and Pi

Quantification of the NAD^+ concentration during preincubation with renal BBMV was performed by luminescence using a high sensitivity NAD/NADH-Glo™ Assay kit (Promega Biotech Ibérica, Madrid, Spain). The experimental samples were prepared exactly as those for Pi uptake, without the addition of Pi for uptake. Samples were obtained at different times up to 30 minutes.

Released Pi was quantified according to the same procedure as for NAD^+/NADH, using a Quantichrom assay kit (BioAssay Systems, Hayward, CA).

Ribosylation assays and antibodies

These assays were performed to determine the activity of the ADP-ribosyltransferases of clostridial toxin-like NAD^+-ADP-ribosyl-Acceptor ADP-ribosyltransferase type C (ARTCs). We exactly followed the protocol previously described for the ^{32}P-ADP-ribosylation of membrane proteins and for detection by autoradiography of SDS-polyacrylamide gel electrophoresis (PAGE) using ^{32}P-NAD^+ from PerkinElmer (Waltham, MA, USA) [32]. Vesicle lysates were clarified by high-speed centrifugation and were subjected to immunoprecipitation with protein G immobilized polyclonal NaPi-IIa or NaPiII-b antibodies. The gels were either dried with a Gel Drier (Bio-Rad, Hercules CA, USA) prior to X-ray exposure, or they were transferred to a polyvinylidene fluoride (PVDF) membrane with a Trans-Blot Turbo (Bio-Rad) for X-ray exposure and Western-blotting. The antibodies for NaPi-IIa have been characterized and described previously [27]. The antibody against NaPi-IIb was obtained from BioWorld (catalogue BS71794, St. Louis Park, MN, USA). For the ribosylation assays, 400 micrograms of BBMV vesicles were used per ribosylation reaction, containing 50 μCi/mL and 10 μM of ^{32}P-NAD^+.

Kinetic analyses and statistics

The kinetic analysis of Pi uptake, the Michalis-Menten saturation assays, and the inhibition calculations were done exactly as previously described in several articles, using Prism 9 (GraphPad Software, San Diego, CA, USA) for Macintosh [10, 33]. In addition, the significances of differences were determined with an analysis of variance and a Tukey's Multiple Comparison Test and were considered significant when $p < 0.05$. All

experiments were performed at least twice (when the results were identical), and the specific number is indicated in the legends of figures, which show a representative experiment.

RESULTS

Effects of NAD^+, NADH, and NAM on Pi transport in BBMV.

The initial experiments sought to characterize the conditions for reproducing and optimizing the inhibition of Pi transport. Rat renal BBMV from kidney cortex were preincubated on ice for 30 minutes with 0.5 mM of either NAD^+, NADH, or NAM. Subsequently, Pi transport was measured for 10 seconds (initial velocity time) while still in the presence of the inhibitors (Figure 2a). Pi uptake was inhibited by approximately 50%, with minimal variations according to the experiment, as shown in the other panels of Figure 2. No inhibition was observed in the absence of preincubation, meaning when the inhibitors were only added to the vesicles at the same time as ^{32}Pi (Figure 2a). This figure also shows that similar results were obtained with BBMV prepared from rat jejunum.

The preincubation temperature did not affect the inhibitory outcome, given that the exact same results were obtained when preincubation took place at either room temperature or on ice (Figure 2b). These results point to a simple binding or interaction rather than requiring an enzymatic reaction, yet the need for preincubation is confusing because it suggests a reaction or at least a complex interaction.

Finally, the specificity of inhibition was confirmed by measuring the effect on the sodium-dependent uptake of D-glucose. Our findings showed an inverse pattern of inhibition compared to Pi: while NAD^+ and NADH did not have an effect, therefore meaning specificity of Pi transport inhibition, NAM did inhibit D-glucose uptake by one third (Figure 2c). While this latter finding is very interesting, we do not have a ready explanation for the effect of NAM on D-glucose transport, and it is beyond the scope of this work.

Effects of NAD^+, NADH, and NAM on Na/Pi cotransporters expressed in *Xenopus laevis* oocytes

In order to check if NAD^+ and NADH were directly inhibiting any of the Pi transporters from the Slc34 and Slc20 families, these transporters were expressed in *Xenopus laevis* oocytes by injecting the corresponding cRNAs. Figure 3 shows the results of 0.5 mM of either NAD^+, NADH, or NAM on the Pi uptake of oocytes expressing the different Pi transporters. Net Pi uptakes are shown. 30 minutes of preincubation with NAD^+, NADH, or NAM was performed at room temperature, and then the uptake of ^{32}Pi was determined for 60 minutes, also in the presence of 0.5 mM of NAD^+, NADH, or NAM. Surprisingly, none of the transporters from the two families were affected by any of the three inhibitors.

Effects of NAD^+, NADH, and NAM on the Na/Pi cotransporter in Opossum Kidney cells and rat cortical nephron segments

The Opossum Kidney (OK) cell line is an excellent *in vitro* model for studying several transport processes of the kidney proximal tubule, including Pi transport/reabsorption [31,34]. We used this cell model to check whether sodium-dependent Pi transport was affected as in the BBMV of kidney cortex and to help understand the NAD^+/NADH mechanism of inhibition. Figure 4 shows that 0.5 mM of NAD^+, NADH, or NAM did not

inhibit Pi uptake in OK cells, regardless of whether the cells were preincubated with the inhibitors. In this case, preincubation was extended up to 3 hours, and the uptake was assayed for 10 minutes, also in the presence of inhibitors.

Based on this unexpected finding of "no effect" and to clarify whether or not the NAD^+/NADH effect on Pi transport was exclusive of the BBMV transport methodology, an ex vivo experiment was performed using proximal tubules purified from rat kidney cortex. Cortical tubules were enzymatically isolated and incubated for 30 minutes with 0.5 mM NAD^+. Immediately after preincubation, BBMV were isolated and Pi uptake was determined. Figure 4d shows, once again, that NAD^+ did not affect the significant sodium dependent Pi uptake observed in BBMV prepared using treated cortical nephron segments.

Kinetic characterization of Pi transport inhibition by NAD^+ and NADH in kidney cortex and jejunum BBMV

Dose-response assays were performed with NAD^+ and NADH in BBMV from the kidney cortex and jejunum of rats, using 50 μM ^{32}Pi as the constant substrate. Figure 5a shows a classic dose-response inhibition, with a small range of concentrations causing uptake to drop. In both tissues, a plateau was reached, and inhibitions were similar at 0.3 and 1 mM of NAD^+ and NADH.

To confirm the competitive mechanism of inhibition previously described using linear transformations [16], several Michaelis, Pi-saturating experiments were performed using kidney cortex BBMV in the presence of several but constant concentrations of NAD^+ (Figure 5b). Non-linear regression fits using a Michaelis-Menten equation plus a non-saturable component showed the effect of increasing the apparent affinity constants, from 0.1 mM in the control condition to 0.23 mM in the presence of 0.3 mM NAD^+ (see right-hand panel). The non-saturable component mainly refers to the unspecific binding of ^{32}Pi to BBMV, and the slope explains the deviation of the fit from a classical Michaelis-Menten curve, which can be determined by mathematical iteration during non-linear regression [10]. A Lineweaver-Burk linear transformation is also shown in Figure 5b (left-hand panel) to illustrate the main effect of NAD^+ on Pi transport: an increase of the apparent Km with an increase of the NAD^+ concentration, suggesting a competitive inhibition. The Km changes are also shown in the right-hand panel of nonlinear regressions. The 2.3-fold increase in Km is enough to cause a theoretical 45% inhibition of Pi uptake, considering a constant Vmax of 206 pmol Pi per milligram of BBMV protein and per second, at the concentration of 0.05 mM Pi, as used in figure 2. Global fits to the different inhibition models were performed. The competitive inhibition model again suggested the kinetic mechanism, providing an apparent K_i of 538 μM NAD^+ in these renal vesicles. In the case of the mixed model of inhibition, the alpha parameter of the model equation turned out to be very large, therefore suggesting that NAD^+ was binding the Pi-free transporter, i.e., behaving like competitive inhibition. The fits corresponding to the different inhibition models were compared according to an extra sum-of-squares F test. This comparison also concluded that the competitive inhibition model was the preferred model.

Role of ribosylation on Pi transport inhibition

To analyze the involvement of ribosylation in the inhibition of Pi transport in BBMV by NAD^+ and NADH, we used several inhibitors of ADP-ribosyltransferases (ART) that could prevent the inhibition of Pi transport. The inhibitors were meta-iodobenzylguanidine (MIBG), novobiocin, vitamins K1 and K3, and 3-methoxybenzamide, which were present during both the preincubation with NAD^+ and the uptake of ^{32}Pi. Figure 6a shows that none of the ART inhibitors used were able to prevent the inhibition of Pi uptake caused by NAD^+.

To confirm the absence of ribosylation as a direct mechanism of Pi transport inhibition, we performed a ribosylation assay using ^{32}P-NAD^+ and BBMV from rat kidney cortex or jejunum. While NaPi-IIa and NaPi-IIb were successfully immunoprecipitated and the ribosylation assay worked for many membrane proteins (see the total ribosylation bands in Figure 6b), neither NaPi-IIa nor NaPi-IIb were ^{32}P-labelled as a consequence of ADP-ribosylation. This is shown in Figure 6b, with the absence of signals in the X-ray films after up to one month of exposure to the blotted membranes.

Metabolism of NAD

The fact that, at least, the ADP-ribosylation of membrane proteins takes place in renal BBMV incubated with NAD^+ (Fig. 6b) suggests a progressive reduction in the concentration of NAD^+ during the 30 minutes of preincubation. This reduction directly affects the apparent Ki value (538 μM NAD^+) determined in the previous section because it should be lower. To ascertain the duration or stability of nicotinamide adenine dinucleotides during the preincubation time, we performed a time-course of the disappearance of NAD^+ from solution in the presence of renal BBMV and on ice. Surprisingly, a very fast decay of NAD^+ concentration was observed, with an exponential-like shape, meaning that the rate of NAD^+ decay seemed to be proportional to the remaining NAD^+ concentration (Fig. 7a). Consequently, a one-phase exponential fit revealed a half-life of approximately two minutes and 2.3 μM NAD^+ at the plateau, meaning that 99.54% of the NAD^+ was consumed during the 30 minutes of preincubation time. More precisely, the initial 500 μM NAD^+ was reduced to 250 μM after 2 minutes, to 90 μM after 5 minutes, to 18 μM after 10 minutes, and to 2.8 μM after 20 minutes.

To check whether other metabolites of NAD^+ could be involved in sodium phosphate cotransport inhibition in renal BBMV, Pi uptake was determined after 30 minutes of preincubation with 500 μM of either niacin, nicotinamide riboside, or adenosine diphosphate ribose (ADP-ribose). Figure 7b shows that, in addition to NAD^+, only ADP-ribose inhibited Pi transport, while niacin and NAM-riboside did not.

Finally, because further metabolism of NAD^+ or ADP-R could lead to the release of free Pi, we also measured the formation of Pi during the 30 minutes of preincubation, with the same conditions as for NAD^+ stability. The results are shown in Fig 7a, revealing a progressive increase of Pi concentration with the preincubation time: up to 0.67 mM when NAD^+ was added to kidney cortex BBMV. This new Pi accumulated during preincubation is therefore acting as a competitive inhibitor during the ^{32}P uptake time (seconds) with BBMV.

DISCUSSION

It is now accepted that nicotinamide is able to control phosphate homeostasis in experimental animals, and this effect takes place after the conversion of NAM into the dinucleotides NAD^+ and NADH [13-15, 23, 34]. However, only a few studies have been performed on human patients [18]. The authors of those studies used different designs and treatment durations, yet they all reported a significant reduction of the Pi concentration in blood. Nevertheless, NAM is not used as a regular drug for CKD, despite the low toxicity of this natural compound [36].

NAD^+ and NADH control Pi homeostasis indirectly, most likely through increased cAMP, redox status, etc. [14, 18, 19, 21, 23]. However, Prof. Thomas Dousa's group reported forty years ago that these dinucleotides also directly inhibit the Pi transport systems located in the apical membranes of intestinal and renal epithelia [15, 16, 24]. In the present work, we have focused on this second mechanism. We have confirmed not only the unexpected apparent competitive inhibition of Pi transport in BBMV (Figure 5b) with non-linear regression kinetic methods, but also the fact that this inhibition requires preincubation with NAD^+ or NADH at either room temperature or on ice, that the inhibition is dose-related (Figure 5a), and that the inhibition is specific for sodium-dependent Pi uptake (Figure 2). However, it can also be concluded that inhibition is not immediately and directly exerted on known Pi transporters because, in addition to the need for preincubation, the Pi transport rates of the transporters expressed in *X. laevis* oocytes were not affected (Figure 3). This was unexpected, as well as the fact that NAD^+ and NADH only inhibited Pi uptake in BBMV, given that they did not affect the renal model of proximal tubule OK cells or even the isolated segments of rat renal cortical nephrons (Figure 4). It is therefore difficult to reconcile the conclusion of a kinetic mechanism of competitive inhibition with no direct interaction with the Pi transporters.

Even though the direct ribosylation of Pi transporters is scarcely compatible with competitive inhibition, we also checked for this, mainly for three reasons. First, it is a reaction that requires NAD^+ or NADH, but not NAM, such as in Pi inhibition. Second, the inhibition of Pi transport also requires preincubation as in ribosylation, and third, incubation during *in vitro* ribosylation reactions can be performed on ice, again as in Pi inhibition (Figure 2) [32]. Given that we were studying the effects on BBMV, we focused on ARTC, namely glycosylphosphatidylinositol (GPI)-anchored membrane proteins (ART1 through ART4). These ecto-ARTCs ADP-ribosylate membrane proteins are present in extracellular body fluids, unlike the intracellular ARTD [37]. Figure 6 shows that, under the same conditions as Pi transport inhibition in BBMV, we did not find evidence of NaPi-IIa or IIb ribosylation. Other ribosylation reactions did take place, however, but on different targets, as shown by the multiple bands of the total lysate sample after exposing the dried polyacrylamide gels to an X-ray film (Figure 6b). It is, nevertheless, very unlikely that the ribosylation of a different target protein is involved in Pi transport inhibition because none of the ribosylation inhibitors used in Figure 6a were able to prevent Pi transport inhibition in renal BBMV.

The competitive inhibition of NAD^+/NADH at the same Pi binding site, as revealed by the kinetic analysis, is surprising for several reasons. First, neither NAM, NAD^+, or NADH affected the type II (Slc34) or type III (Slc20) transporters expressed in *X. laevis* oocytes (Figure 3). Also, OK cells, which strongly express NaPi-IIa and NaPi-IIc, or even the cortical nephron segments (Figure 4) were unaffected. In a previous study, NAM reduced the expression of NaPi-IIa (NaPi-4) in OK cells only after overexpression of Nampt, but direct inhibition by NAD^+ or NADH was not reported [13]. Second, direct competitive inhibition of the transporters (i.e., competition with the binding site of Pi in the transporters) would also be unusual because the chemical structure of these compounds is unrelated to that of orthophosphoric acid. However, this possibility cannot be discarded because other reported competitive inhibitors also exhibit very different structures [10].

The binding of NAD^+ to renal BBMV does take place, however. It was first described and characterized in 1983 [24] as a true binding rather than the uptake of NAD, with two kinetically distinct binding sites characterized by dissociation constants in the micromolar and millimolar range, respectively. For the assay, the authors used [adenine-2,8-^{3}H]NAD^+. The need for the extravesicular presence of NAD was confirmed afterwards [38]. Binding is a requisite for reactions in which these dinucleotides are involved, and it dictates the fate of NAD^+/NADH. For example, in addition to the post-translational modification of proteins by ribosylation, NAD^+-dependent protein deacetylation and NAD^+/NADH binding to redox sensors proteins should be considered [39]. From these three functions, only redox status has been described as a modulator of Pi transport via NAD^+/NADH [21]. NAD^+ binds to many other plasma membrane proteins, such as the ubiquitous NAD glycohydrolase CD38 [40] or several ion channels that contain Rossmann folds [39, 41]. Binding should take place on a membrane protein that regulates these transporters, but such a membrane protein is not endogenously expressed in *X. laevis* oocytes or in OK cells, unless these cells are able to neutralize binding or the effects of binding, for example by uptaking NAD^+ after binding, as stated above. Nevertheless, this is not a usual competitive inhibition mechanism because ^{32}Pi is not present during the preincubation time, but rather during the 10 seconds of ^{32}Pi uptake (initial velocity).

Either ribosylation through PARPs/ARTCs, or deacetylation through sirtuins, or the glycohydrolase activity of CD38 and other enzymes causes the degradation of NAD^+/NADH and the formation of ADP-ribose or variants thereof (acetyl-ADPR, cyclic ADPR, etc.) [42]. Consequently, we quantified the persistence of the initial concentration of NAD^+/NADH during the 30 minutes of preincubation time and surprisingly found that the half-life was only two minutes (Fig. 7a). This rapid vanishing is very important when interpreting the results, not only because it prevents NAD^+/NADH from direct binding to the Pi transporters but also because preincubation should not be necessary, given that incubation with BBMV lasts only ten seconds. Therefore, some metabolite(s) of NAD^+/NADH degradation should be involved, and NAM was discarded from the first experiments. We therefore checked NAM-ribose and, especially, ADP-ribose, in addition to niacin (Fig. 7b), which revealed that ADPR inhibited just as much as NAD^+/NADH. We did not measure the formation of ADPR during the preincubation time, but either ADPR or NAD^+/NADH could result in the formation of Pi by end

hydrolysis of ADP. Therefore, we measured Pi formation during the preincubation time, revealing a steady increase (Fig. 7a). The formation of Pi, either directly or indirectly, could explain the competitive inhibition observed in BBMV and the need for preincubation leading to the accumulation of free Pi in the uptake medium, which would act as an inhibitor of ^{32}Pi uptake. It is still unclear whether this is the only mechanism or if additional compounds such as ADPR are participating in the inhibition of Pi transport. However, the fact that this inhibition only occurs in BBMV (i.e., NAD^+ and NADH are not able to affect Pi uptake in OK cells, in isolated nephron segments of kidney cortex, or in *Xenopus laevis* oocytes expressing Pi transporters) suggests a limited relevance of the direct effect of NAD^+/NADH in Pi transporters *in vivo* but a strong effect by these compounds, as well as by NAM, in the control of Pi homeostasis, as described [13,14].

GRANTS

This research was funded by the Ministerio de Ciencia, Innovación y Universidades with grant number PGC2018-098635-B-I00. S.L. was a recipient of a predoctoral fellowship from the Government of Aragon (IIU/1/2017).

DISCLOSURES

No conflicts of interest, financial or otherwise, are declared by the authors.

REFERENCES

1. Levi M, Gratton E, Forster IC, Hernando N, Wagner CA, Biber J, Sorribas V, Murer H. Mechanisms of phosphate transport. ***Nat Rev Nephrol*** 15: 482-500, 2019. doi: 10.1038/s41581-019-0159-y
2. Hernando N, Gagnon K, Lederer E. Phosphate Transport in Epithelial and Nonepithelial Tissue. ***Physiol Rev*** 10: 1-35, 2021. doi: 10.1152/physrev.00008.2019
3. Magagnin S, Werner A, Markovich D, Sorribas V, Stange G, Biber J, Murer H. Expression cloning of human and rat renal cortex Na/Pi cotransport. ***Proc Natl Acad Sci U S A*** 90: 5979–5983, 1993. doi: 10.1073/pnas.90.13.5979.
4. Hilfiker H, Hattenhauer O, Traebert M, Forster I, Murer H, Biber J. Characterization of a murine type II sodium-phosphate cotransporter expressed in mammalian small intestine. ***Proc Natl Acad Sci USA*** 95: 14564–14569, 1998. doi: 10.1073/pnas.95.24.14564.
5. Segawa H, Kaneko I, Takahashi A, Kuwahata M, Ito M, Ohkido I, Tatsumi S, Miyamoto K. Growth-related renal type II Na/Pi cotransporter. ***J Biol Chem*** 277: 19665–19672, 2002. doi: 10.1074/jbc.M200943200.
6. Kavanaugh, M.P., Miller, D.G., Zhang, W., Law, W., Kozak, S.L., Kabat, D., Miller, A.D. Cell-surface receptors for gibbon ape leukemia virus and amphotropic murine retrovirus are inducible sodium-dependent phosphate symporters. ***Proc. Natl. Acad. Sci. USA*** 91: 7071–7075, 1994. doi: 10.1073/pnas.91.15.7071.
7. Olah, Z., Lehel, C., Anderson, W.B., Eiden, M.V., Wilson, C.A. The cellular receptor for gibbon ape leukemia virus is a novel high affinity sodium dependent phosphate transporter. ***J Biol Chem*** 269: 25426–25431, 1994.
8. Komaba H, Fukagawa M. Phosphate-A poison for humans? ***Kidney Int***. 90: 753-763, 2016. doi: 10.1016/j.kint.2016.03.039.
9. Shiizaki K, Tsubouchi A, Miura Y, Seo K, Kuchimaru T, Hayashi H, Iwazu Y, Miura M, Battulga B, Ohno N, Hara T, Kunishige R, Masutani M, Negishi K, Kario K, Kotani K, Yamada T, Nagata D, Komuro I, Itoh H, Kurosu H, Murata M, Kuro-O M. Calcium phosphate microcrystals in the renal tubular fluid accelerate chronic kidney disease progression. ***J Clin Invest*** 131:e145693, 2021. doi: 10.1172/JCI145693.
10. Sorribas V, Guillén N, Sosa C. Substrates and inhibitors of phosphate transporters: from experimental tools to pathophysiological relevance. ***Pflugers Arch*** 471: 53-65, 2019. doi: 10.1007/s00424-018-2241-x.
11. Hill Gallant KM, Stremke ER, Trevino LL, Moorthi RN, Doshi S, Wastney ME, Hisada N, Sato J, Ogita Y, Fujii N, Matsuda Y, Kake T, Moe SM. EOS789, a broad-spectrum inhibitor of phosphate transport, is safe with an indication of efficacy in a phase 1b randomized crossover trial in hemodialysis patients. ***Kidney Int*** 99: 1225-1233, 2021. doi: 10.1016/j.kint.2020.09.035.
12. Liu L, Su X, Quinn WJ 3rd, Hui S, Krukenberg K, Frederick DW, Redpath P, Zhan L, Chellappa K, White E, Migaud M, Mitchison TJ, Baur JA, Rabinowitz JD. Quantitative Analysis of NAD Synthesis-Breakdown Fluxes. ***Cell Metab*** 27: 1067-1080.e5, 2018. doi: 10.1016/j.cmet.2018.03.018.

13. Nomura K, Tatsumi S, Miyagawa A, Shiozaki Y, Sasaki S, Kaneko I, Ito M, Kido S, Segawa H, Sano M, Fukuwatari T, Shibata K, Miyamoto K. Hepatectomy-related hypophosphatemia: a novel phosphaturic factor in the liver-kidney axis. ***J Am Soc Nephrol*** 25: 761-772, 2014. doi: 10.1681/ASN.2013060569.
14. Miyagawa A, Tatsumi S, Takahama W, Fujii O, Nagamoto K, Kinoshita E, Nomura K, Ikuta K, Fujii T, Hanazaki A, Kaneko I, Segawa H, Miyamoto KI. The sodium phosphate cotransporter family and nicotinamide phosphoribosyltransferase contribute to the daily oscillation of plasma inorganic phosphate concentration. ***Kidney Int*** 93*:* 1073-1085, 2018. doi: 10.1016/j.kint.2017.11.022
15. Kempson SA, Colon-Otero G, Ou SY, Turner ST, Dousa TP. Possible role of nicotinamide adenine dinucleotide as an intracellular regulator of renal transport of phosphate in the rat. ***J Clin Invest*** 67: 1347-1360, 1981. doi: 10.1172/jci110163.
16. Kempson SA, Turner ST, Yusufi AN, Dousa TP. Actions of NAD+ on renal brush border transport of phosphate in vivo and in vitro. ***Am J Physiol*** 249: F948-F955, 1985. doi: 10.1152/ajprenal.1985.249.6.F948.
17. Katai K, Tanaka H, Tatsumi S, Fukunaga Y, Genjida K, Morita K, Kuboyama N, Suzuki T, Akiba T, Miyamoto K, Takeda E. Nicotinamide inhibits sodium-dependent phosphate cotransport activity in rat small intestine. ***Nephrol Dial Transplant*** 14: 1195-1201, 1999. doi: 10.1093/ndt/14.5.1195.
18. Eto N, Miyata Y, Ohno H, Yamashita T. Nicotinamide prevents the development of hyperphosphataemia by suppressing intestinal sodium-dependent phosphate transporter in rats with adenine-induced renal failure. ***Nephrol Dial Transplant*** 20: 1378-1384, 2005. doi: 10.1093/ndt/gfh781.
19. Campbell PI, Abraham MI, Kempson SA. Increased cAMP in proximal tubules is acute effect of nicotinamide analogues. ***Am J Physiol*** 257 F1021- F1026, 1989. doi: 10.1152/ajprenal.1989.257.6.F1021.
20. Campbell PI, al-Mahrouq HA, Abraham MI, Kempson SA. Specific inhibition of rat renal Na+/phosphate cotransport by picolinamide. ***J Pharmacol Exp Ther*** 251: 188-192, 1989.
21. Suzuki M, Capparelli AW, Jo OD, Yanagawa N. Thiol redox and phosphate transport in renal brush-border membrane. Effect of nicotinamide. ***Biochim Biophys Acta*** 1021: 85-90, 1990. doi: 10.1016/0005-2736(90)90388-5.
22. Berndt TJ, Pfeifer JD, Knox FG, Kempson SA, Dousa TP. Nicotinamide restores phosphaturic effect of PTH and calcitonin in phosphate deprivation. ***Am J Physiol*** 242: F447-F452, 1982. doi: 10.1152/ajprenal.1982.242.5.F447.
23. Haas JA, Berndt TJ, Haramati A, Knox FG. Nephron sites of action of nicotinamide on phosphate reabsorption. ***Am J Physiol*** 246: F27-F31, 1984. doi: 10.1152/ajprenal.1984.246.1.F27.
24. Braun-Werness JL, Jackson BA, Werness PG, Dousa TP. Binding of nicotinamide adenine dinucleotide by the renal brush border membrane from rat kidney cortex. ***Biochim Biophys Acta*** *732*,553-561, 1983. doi: 10.1016/0005-2736(83)90231-6.
25. Biber J, Stieger B, Stange G, Murer H. Isolation of renal proximal tubular brush-border membranes. ***Nat Protoc*** 2: 1356–1359, 2007. doi:10.1038/nprot.2007.156.

26. Giral H, Caldas Y, Sutherland E, Wilson P, Breusegem S, Barry N, Blaine J, Jiang T, Wang XX, Levi M. Regulation of rat intestinal Na-dependent phosphate transporters by dietary phosphate. ***Am J Physiol Renal Physiol*** 297: F1466–F1475, 2009. doi:10.1152/ajprenal.00279.2009.
27. Villa-Bellosta R, Ravera S, Sorribas V, Stange G, Levi M, Murer H, Biber J, Forster IC. The Na+-Pi cotransporter PiT-2 (SLC20A2) is expressed in the apical membrane of rat renal proximal tubules and regulated by dietary Pi. ***Am J Physiol Renal Physiol*** 296: F691-F692, 2009. doi: 10.1152/ajprenal.90623.2008.
28. Schafer JA, Watkins ML, Li L, Herter P, Haxelmans S, Schlatter E. A simplified method for isolation of large numbers of defined nephron segments. ***Am J Physiol*** 273:F650-F657, 1997. doi: 10.1152/ajprenal.1997.273.4.F650.
29. Villa-Bellosta R, Bogaert YE, Levi M, Sorribas V. Characterization of phosphate transport in rat vascular smooth muscle cells: implications for vascular calcification. ***Arterioscler Thromb Vasc Biol*** 27: 1030-1036, 2007. doi: 10.1161/ATVBAHA.106.132266
30. Villa-Bellosta R, Sorribas V. Role of rat sodium/phosphate cotransporters in the cell membrane transport of arsenate. ***Toxicol Appl Pharmacol***, 232: 125-134, 2008. doi: 10.1016/j.taap.2008.05.026.
31. Guillén N, Caldas YA, Levi M, Sorribas V. Identification and expression analysis of type II and type III P(i) transporters in the opossum kidney cell line. ***Exp Physiol*** 104: 149-161, 2019. doi: 10.1113/EP087217.
32. Menzel S, Adriouch S, Bannas P, Haag F, Koch-Nolte F. Monitoring Expression and Enzyme Activity of Ecto-ARTCs. ***Methods Mol Biol*** 1813: 167-186, 2018. doi: 10.1007/978-1-4939-8588-3_11.
33. Hortells L, Guillén N, Sosa C, Sorribas V. Several phosphate transport processes are present in vascular smooth muscle cells. ***Am J Physiol Heart Circ Physiol*** 318: H448-H460, 2020. doi: 10.1152/ajpheart.00433.2019.
34. Sorribas V, Markovich D, Hayes G, Stange G, Forgo J, Biber J, Murer H. Cloning of a Na/Pi cotransporter from opossum kidney cells. ***J Biol Chem*** 269: 6615-6621, 1994.
35. Wu KI, Bacon RA, Al-Mahrouq HA, Kempson SA. Nicotinamide as a rapid-acting inhibitor of renal brush-border phosphate transport. ***Am J Physiol***, 255: F15-F21, 1988. doi: 10.1152/ajprenal.1988.255.1.F15.
36. Ginsberg C, Ix JH. Nicotinamide and phosphate homeostasis in chronic kidney disease. ***Curr Opin Nephrol Hypertens***, 25: 285-291, 2016. doi: 10.1097/MNH.0000000000000236.
37. Cohen MS, Chang P. Insights into the biogenesis, function, and regulation of ADP-ribosylation. ***Nat Chem Biol***: 14: 236-243, 2018. doi: 10.1038/nchembio.2568.
38. Gmaj P, Biber J, Angielski S, Stange G, Murer H. Intravesicular NAD has no effect on sodium-dependent phosphate transport in isolated renal brush border membrane vesicles. ***Pflugers Arch*** 400: 60-65 1984. doi: 10.1007/BF00670537.
39. Koch-Nolte F, Fischer S, Haag F, Ziegler M. Compartmentation of NAD^+-dependent signalling. ***FEBS Lett 585***, 1651-1656, 2011. doi: 10.1016/j.febslet.2011.03.045

40. Wolters V, Rosche A, Bauche A, Kulow F, Harneit A, Fliegert R, Guse AH. NAD binding by human CD38 analyzed by Trp189 fluorescence. ***Biochim Biophys Acta Mol Cell Res*** 1866: 1189-1196, 2019. doi: 10.1016/j.bbamcr.2018.11.011
41. Kilfoil PJ, Tipparaju SM, Barski OA, Bhatnagar A. Regulation of ion channels by pyridine nucleotides. ***Circ Res*** 112: 721-741, 2013. doi: 10.1161/CIRCRESAHA.111.247940.
42. Covarrubias AJ, Perrone R, Grozio A, Verdin E. NAD^+ metabolism and its roles in cellular processes during ageing. ***Nat Rev Mol Cell Biol*** 22:119-141, 2021. doi: 10.1038/s41580-020-00313-x

FIGURE CAPTIONS

Figure 1. Chemical structures of nicotinamide-related compounds. Top, the three vitamers of vitamin B_3 and the metabolite ADP-Ribose. Bottom, interconversion of NADH and NAD^+ by redox reactions.

Figure 2. Effects of preincubation and temperature on NAD^+, NADH, and NAM inhibition of Pi uptake. (**a**) Comparison of the effect on Pi uptake by the indicated chemicals (all three at 0.5 mM) due to 30 minutes of ice-cold preincubation (left) vs. no preincubation (right) of BBMV from kidney cortex (top) and jejunum (bottom). (**b**) Effect of temperature, during the 30 minutes of preincubation, on Pi uptake in kidney cortex BBMV. (**c**) Specificity of NAD^+/NADH preincubation effects on Pi transport in kidney BBMV. During the incubation for ^{32}Pi uptake, the assayed compounds were also present in the uptake media. All experiments were performed twice, and asterisks mean a significant difference compared to the control condition with an ANOVA and a Tukey's multiple comparison test. *$p < 0.05$; **$p < 0.01$; ***$p < 0.001$.

Figure 3. Effect of NAD^+, NADH, and NAM on oocytes expressing rat Na/Pi cotransporters. *Xenopus laevis* oocytes were injected with 5 ng of the indicated transporter cRNAs, and after 3 days the effect of 30 minutes of preincubation with 0.5 mM of NAD^+, NADH, or NAM was assayed. Uptake of ^{32}Pi was determined after one hour of incubation in the presence of the same compound used during preincubation. Net Pi uptakes are shown. All experiments were performed twice with identical results, and no significant effects were observed in any of the type II (Slc34 members) or type III (Slc20) Pi transporters, or in the water-injected oocytes, with an ANOVA and a Tukey's multiple comparison post-test.

Figure 4. Effect of nicotinamide derivatives on Pi uptake in live cells. OK cells were preincubated for 0 minutes (a), 30 minutes (b), and 3 hours (c) with 0.5 mM of NAD^+, NADH, and NAM, and then the cells were assayed for ^{32}P uptake. Uptake media contained the corresponding compound used during preincubation. No significant effect was observed for up to 3 hours of preincubation. (d) NAD^+ was also assayed in proximal tubules isolated from rat kidney cortex. The tubules were incubated for 30 minutes with 0.5 mM NAD^+, and BBMV were then immediately isolated and Pi transport was determined for 10 seconds. A robust sodium dependent Pi transport was observed (white bars) compared to uptake in the absence of sodium (grey bars), but NAD^+ again did not affect that Pi transport.

Figure 5. Kinetic analysis of NAD^+ and NADH inhibition of Pi uptake in kidney cortex BBMV. (**a**) Dose-response relationship of NAD^+ and NADH on BBMV Pi uptake. The effect of preincubation with increasing concentrations of NAD^+ and NADH on intestinal and renal BBMV is shown. Pi concentration was kept constant at 0.05 mM, and nonlinear regression lines were obtained after fitting a dose-response equation to data. (**b**) The inhibitory effect of different concentrations of NAD^+ on Pi uptake was assayed in the presence of increasing concentrations of Pi. Left, linear regressions of Lineweaver-Burk transformations to show the effect

on Pi transport K_m (where lines cross the abscissas, the values correspond to 1/Km). The large chart shows the details, with the complete chart shown as an inset. Right, nonlinear regression curves after fitting a Michaelis-Menten equation to the data, containing a non-saturable component (related to the unspecific binding and diffusion of ^{32}Pi). The apparent K_i value was obtained with a global fit sharing the rest of the parameters (see text for details). The legends indicate the K_m values, which are also shown where they intersect with the abscissa axis. The large chart shows the details up to 1 mM Pi on the abscissas. The inset shows the theoretical Michaelis curves after eliminating the non-saturable (Kd*[S]) component, in the complete range of abscissa concentrations used (up to 6 mM Pi).

Figure 6. Role of ribosylation on Pi transport inhibition. (**a**) Effect of ART inhibitors on the NAD^+ effect on Pi uptake in renal BBMV. The inhibitors were present simultaneously with 0.5 mM NAD^+ during the preincubation and uptake times. In two different experiments, neither of them prevented the NAD^+ effect, and the levels of all the Pi uptake conditions were significantly different (***$p < 0.001$) from the control (ANOVA). MIBG, meta-iodobenzylguanidine. Novob, novobiocin. 3-MB, 3-Methoxybenzamide. (**b**) *In vitro* ribosylation assays of Pi transporters. Rat BBMV from jejunum or kidney cortex were ribosylated using ^{32}P-NAD^+. Left, total ^{32}P-ribosylation of BBMV proteins previous to immunoprecipitation. Middle, after the immunoprecipitation of NaPi-IIa or NaPi-IIb proteins from ribosylated kidney cortex or jejunum BBMV, respectively. The samples were electrophoresed, and the gels were then blotted onto membranes and exposed to X-ray films at -80º C for up to one month. No evidence of ^{32}P signals was observed. Right, the same membranes were then immunoprobed against NaPi-IIa or NaPi-IIb, revealing the presence of both non-ribosylated Pi transporters.

Figure 7. NAD^+ metabolism in BBMV. (**a**) Disappearance of NAD^+ during the 30 minutes of preincubation with kidney BBMV, under the same conditions as those for Pi transport uptake. In parallel, free Pi is increase (**b**) No effect of 0.5 mM niacin or nicotinamide riboside preincubations on Pi uptake by kidney BBMV. ADP ribose inhibited similarly to NAD^+. The experiments were performed twice with similar results. Asterisks mean a significant difference compared to the control condition with an ANOVA and a Tukey's multiple comparison test. ***$p < 0.001$.

Figure 1

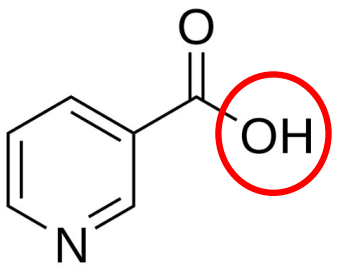

Niacin
(nicotinic acid)

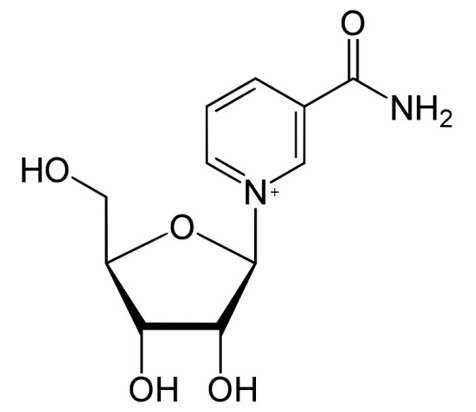

Nicotinamide riboside

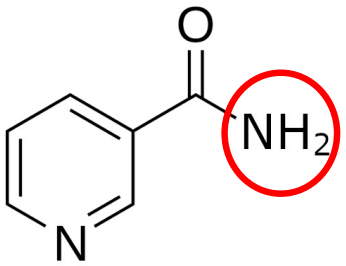

Nicotinamide

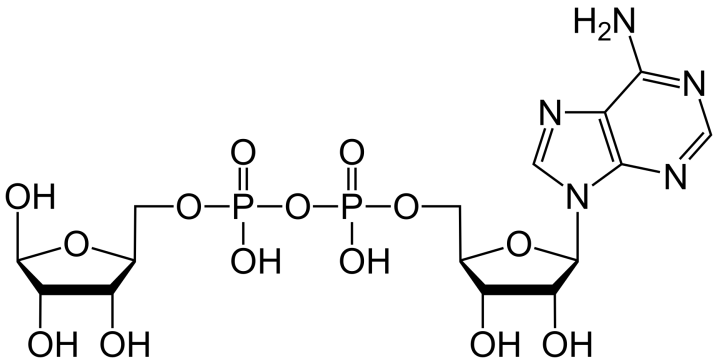

ADP-ribose

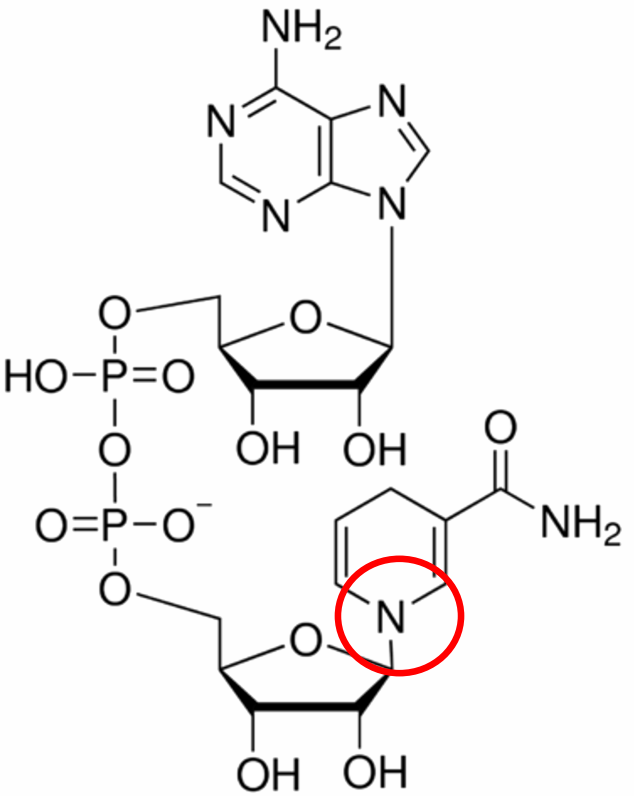

NADH

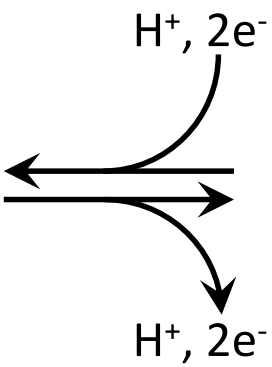

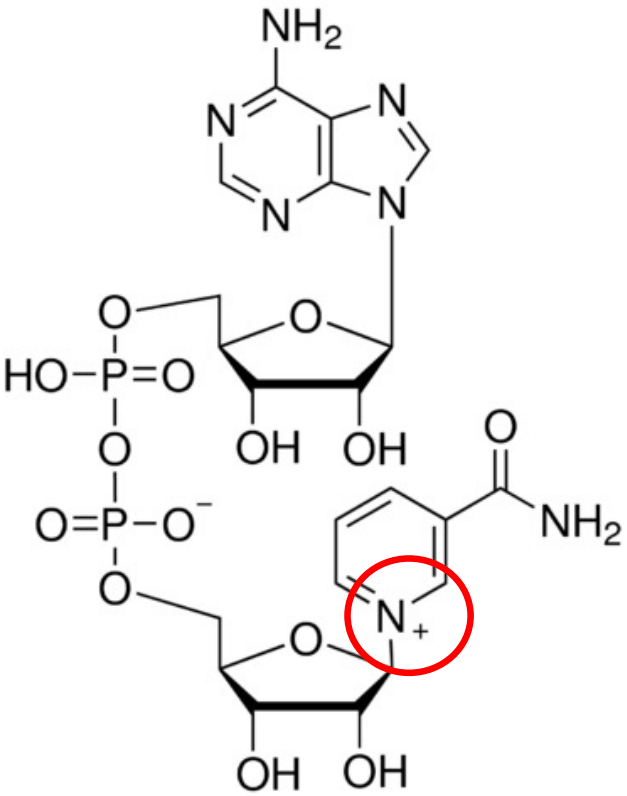

NAD+

Figure 2

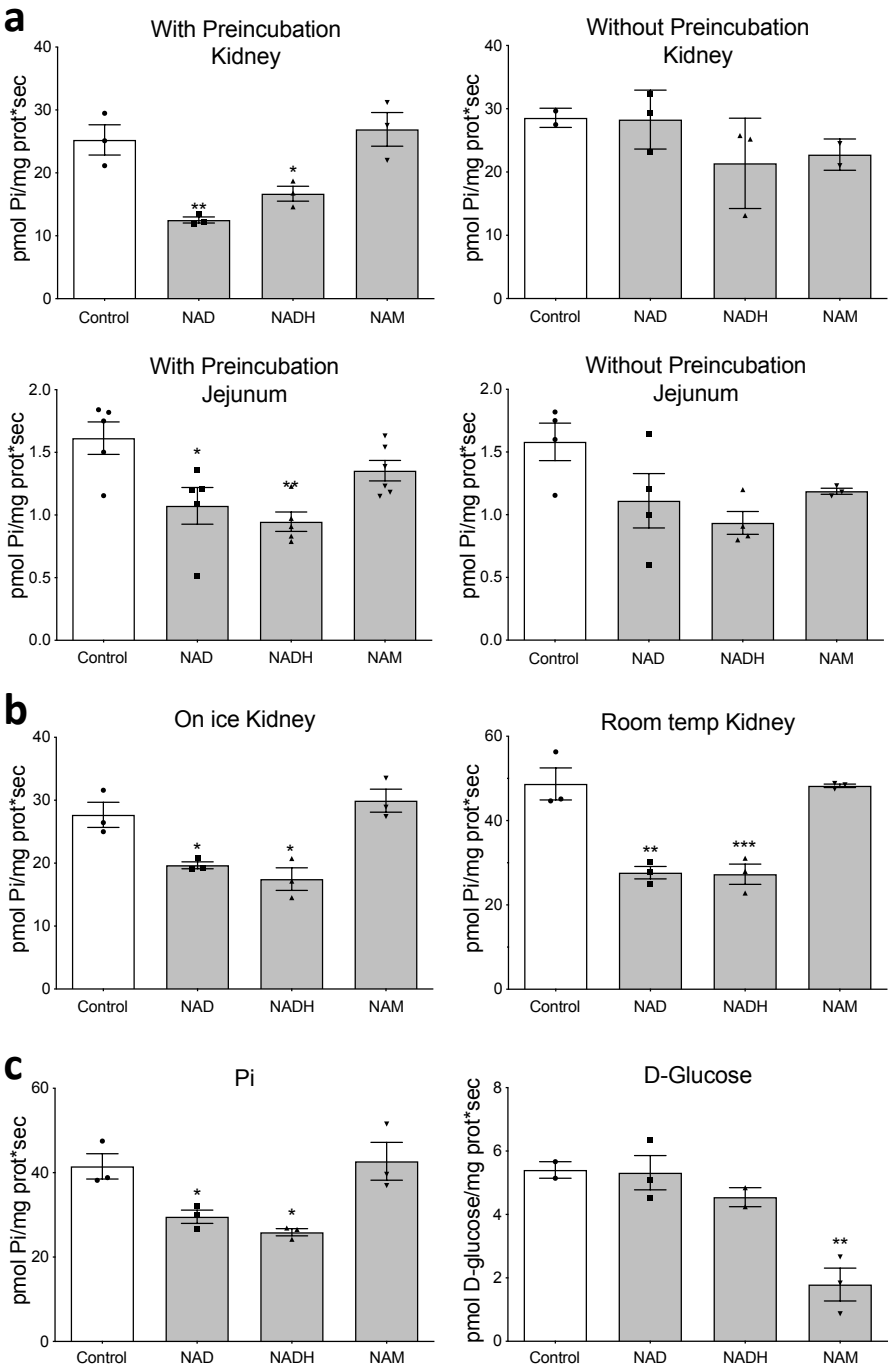
a
With Preincubation
Kidney
Without Preincubation
Kidney
With Preincubation
Jejunum
Without Preincubation
Jejunum
pmol Pi/mg prot*sec
Control
NAD
NADH
NAM
b
On ice Kidney
Room temp Kidney
c
Pi
D-Glucose
pmol D-glucose/mg prot*sec

Figure 3

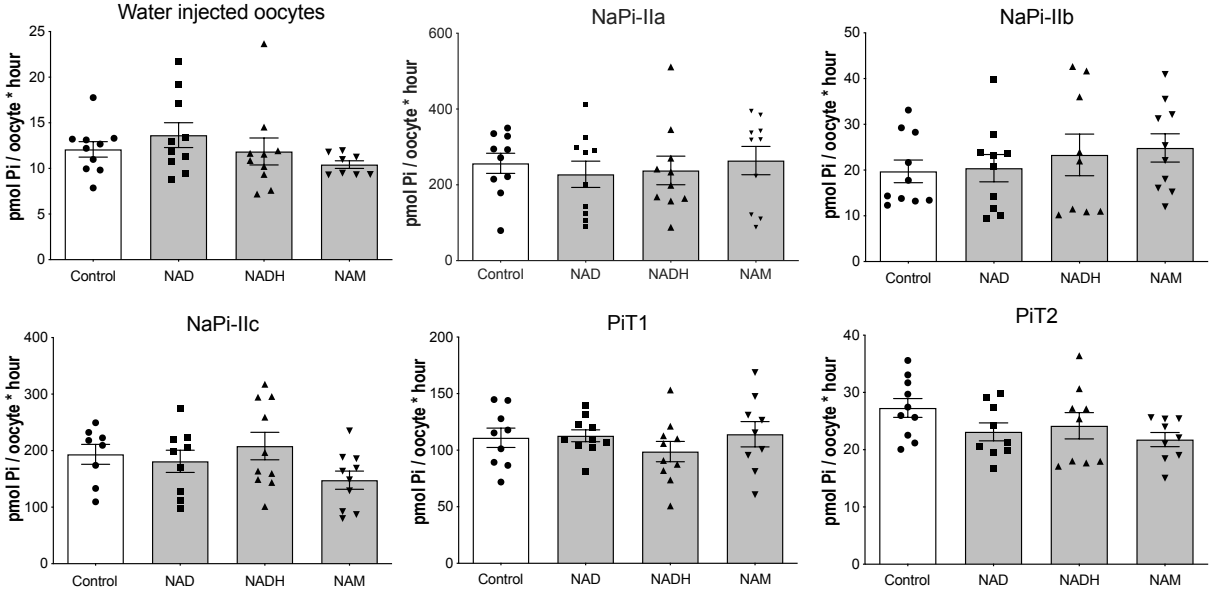
Water injected oocytes
NaPi-IIa
NaPi-IIb
NaPi-IIc
PiT1
PiT2
pmol Pi / oocyte * hour
Control
NAD
NADH
NAM

Figure 4

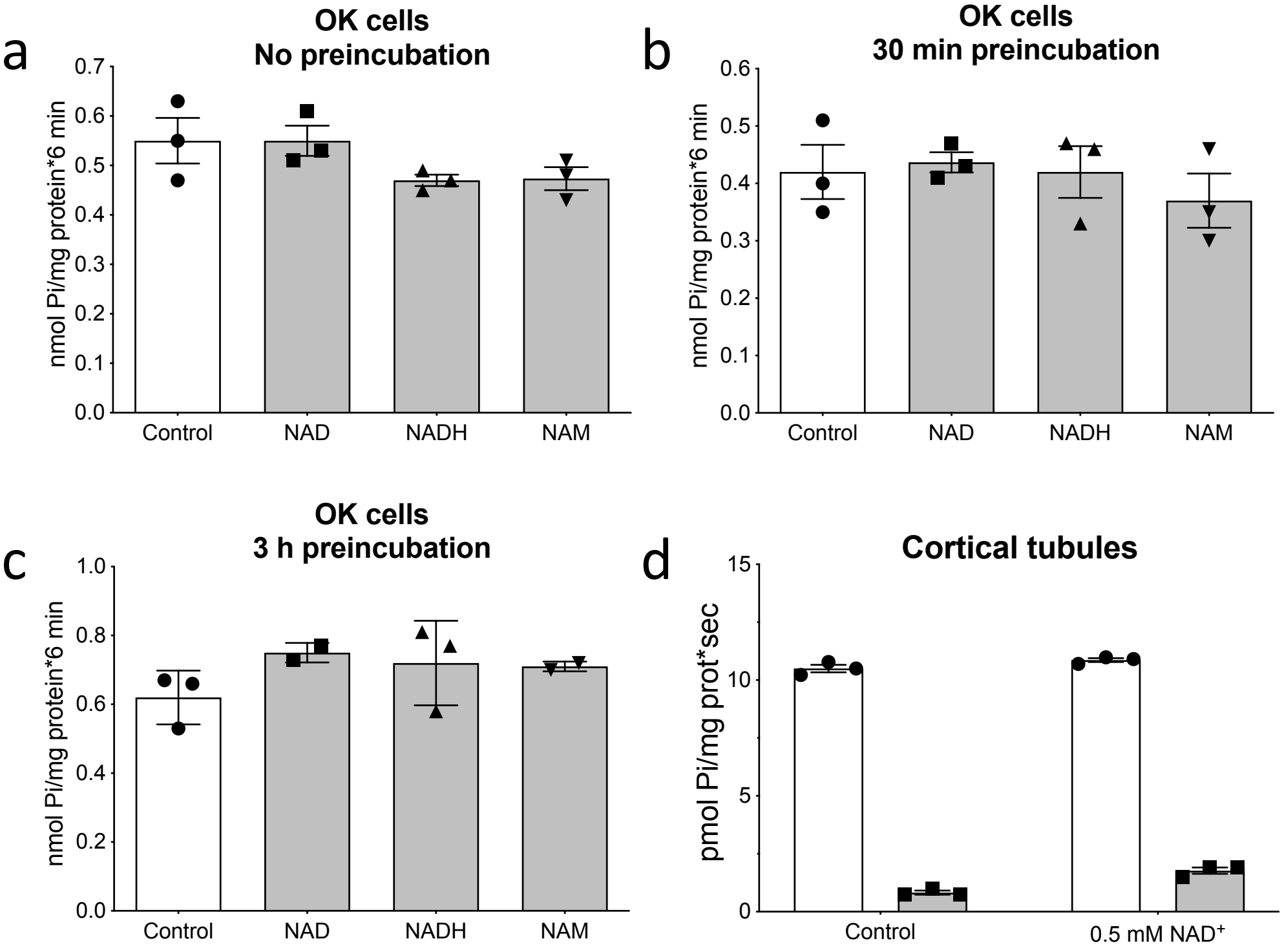
a
OK cells
No preincubation
nmol Pi/mg protein*6 min
0.0
0.1
0.2
0.3
0.4
0.5
0.6
0.7
Control
NAD
NADH
NAM
b
OK cells
30 min preincubation
nmol Pi/mg protein*6 min
0.0
0.1
0.2
0.3
0.4
0.5
0.6
Control
NAD
NADH
NAM
c
OK cells
3 h preincubation
nmol Pi/mg protein*6 min
0.0
0.2
0.4
0.6
0.8
1.0
Control
NAD
NADH
NAM
d
Cortical tubules
pmol Pi/mg prot*sec
0
5
10
15
Control
0.5 mM NAD+

Figure 5

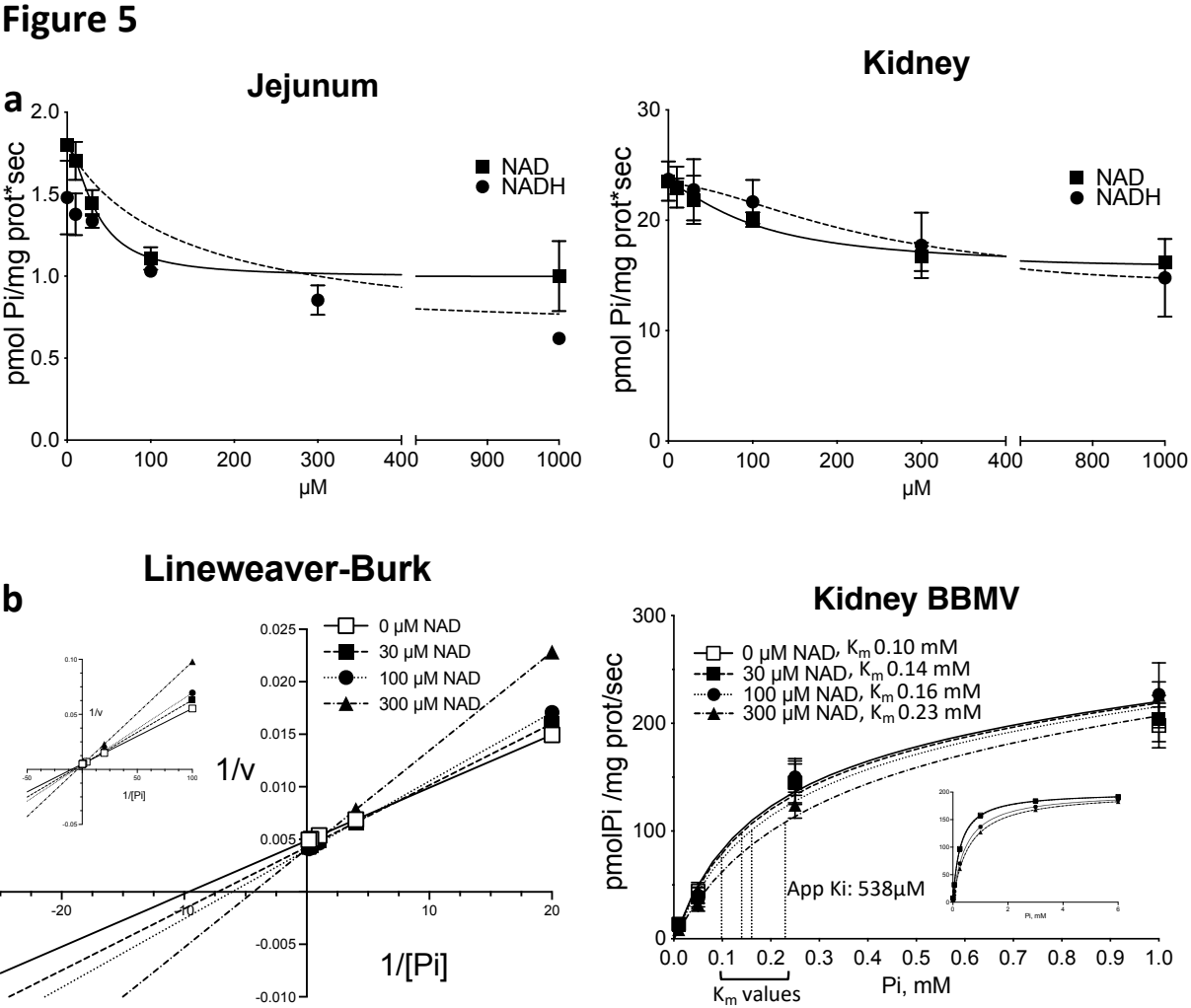
a
Jejunum
pmol Pi/mg prot*sec
NAD
NADH
μM
Kidney
pmol Pi/mg prot*sec
NAD
NADH
μM
b
Lineweaver-Burk
0 μM NAD
30 μM NAD
100 μM NAD
300 μM NAD
1/v
1/[Pi]
Kidney BBMV
pmolPi /mg prot/sec
0 μM NAD, Km 0.10 mM
30 μM NAD, Km 0.14 mM
100 μM NAD, Km 0.16 mM
300 μM NAD, Km 0.23 mM
App Ki: 538μM
Km values
Pi, mM

Figure 6

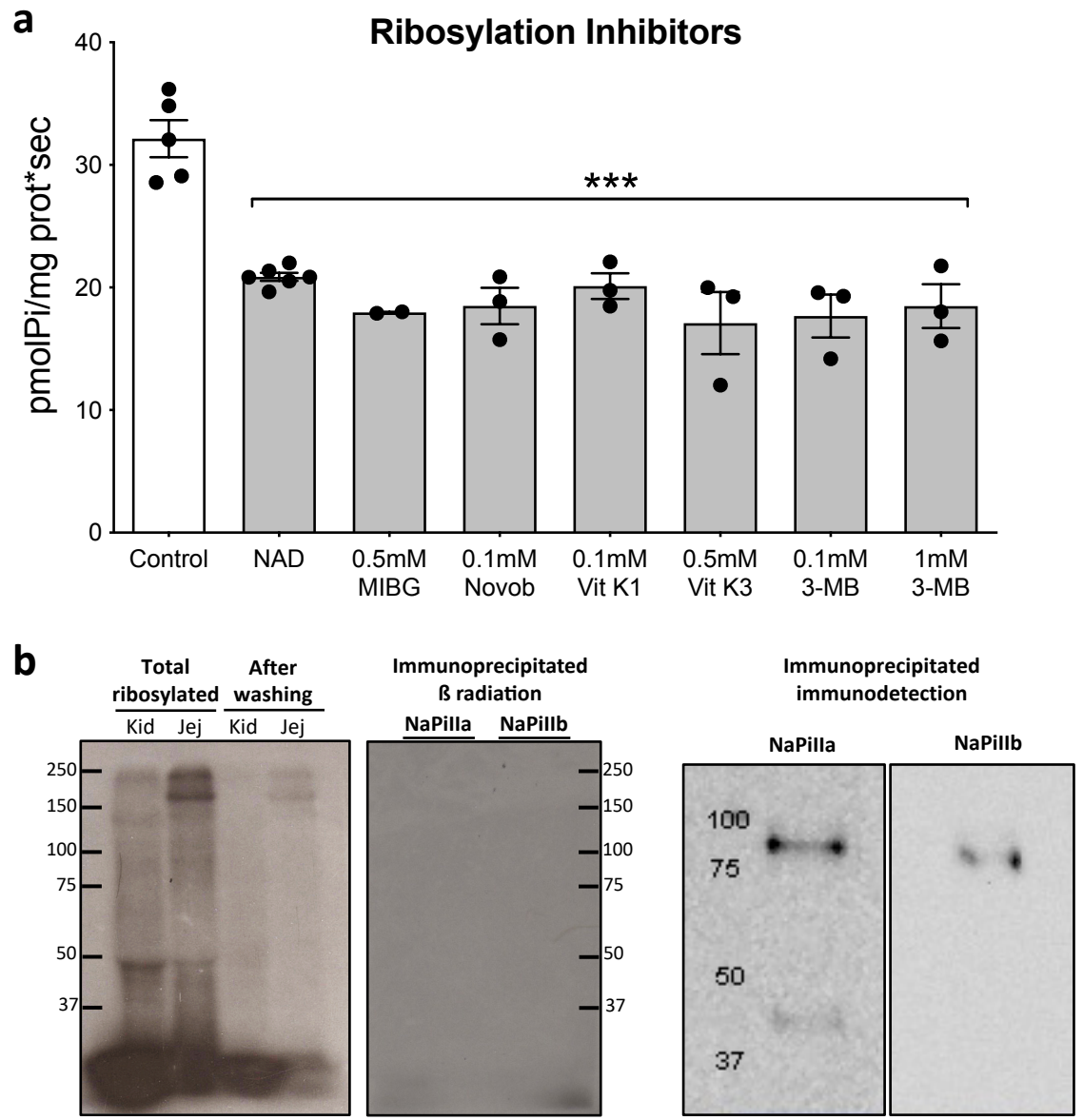
a
Ribosylation Inhibitors
pmolPi/mg prot*sec
40
30
20
10
0
***
Control
NAD
0.5mM MIBG
0.1mM Novob
0.1mM Vit K1
0.5mM Vit K3
0.1mM 3-MB
1mM 3-MB
b
Total ribosylated
After washing
Kid
Jej
Kid
Jej
250
150
100
75
50
37
Immunoprecipitated ß radiation
NaPiIIa
NaPiIIb
250
150
100
75
50
37
Immunoprecipitated immunodetection
NaPiIIa
NaPiIIb
100
75
50
37

Figure 7

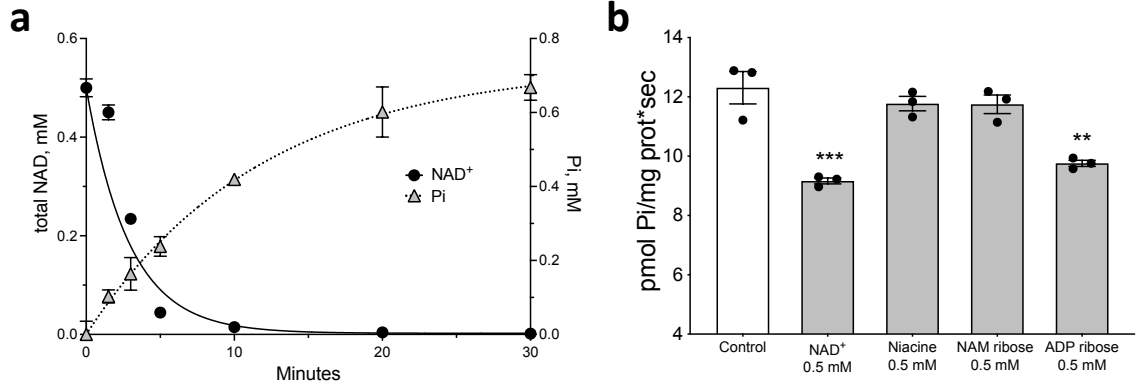
a
total NAD, mM
Pi, mM
Minutes
NAD+
Pi
0.0
0.2
0.4
0.6
0.8
0
10
20
30
b
pmol Pi/mg prot*sec
4
6
8
10
12
14
***
**
Control
NAD+ 0.5 mM
Niacine 0.5 mM
NAM ribose 0.5 mM
ADP ribose 0.5 mM